

Experimentally Validated hERG Pharmacophore Models as Cardiotoxicity Prediction Tools

Jadel M. Kratz,^{†,‡} Daniela Schuster,^{*,§} Michael Edtbauer,[§] Priyanka Saxena,^{||} Christina E. Mair,[‡] Julia Kirchbner,[§] Barbara Matuszczak,[§] Igor Baburin,^{||} Steffen Hering,^{||} and Judith M. Rollinger^{*,‡}

[†]Departamento de Ciências Farmacêuticas, Universidade Federal de Santa Catarina, 88.040-900 Florianópolis, Santa Catarina, Brazil

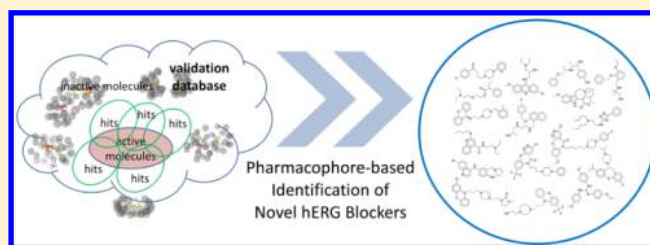
[‡]Institute of Pharmacy/Pharmacognosy and Center for Molecular Biosciences Innsbruck, University of Innsbruck, Innrain 80-82, 6020 Innsbruck, Austria

[§]Institute of Pharmacy/Pharmaceutical Chemistry and Center for Molecular Biosciences Innsbruck, University of Innsbruck, Innrain 80-82, 6020 Innsbruck, Austria

^{||}Department of Pharmacology and Toxicology, University of Vienna, Althanstraße 14, 1090 Vienna, Austria

Supporting Information

ABSTRACT: The goal of this study was to design, experimentally validate, and apply a virtual screening workflow to identify novel hERG channel blockers. The hERG channel is an important antitarget in drug development since cardiotoxic risks remain as a major cause of attrition. A ligand-based pharmacophore model collection was developed and theoretically validated. The seven most complementary and suitable models were used for virtual screening of in-house and commercially available compound libraries. From the hit lists, 50 compounds were selected for experimental validation through bioactivity assessment using patch clamp techniques. Twenty compounds inhibited hERG channels expressed in HEK 293 cells with IC_{50} values ranging from 0.13 to 2.77 μ M, attesting to the suitability of the models as cardiotoxicity prediction tools in a preclinical stage.



■ INTRODUCTION

The human ether-a-go-go-related gene (hERG) channel plays a critical role in cardiac action potential repolarization. Its importance was amplified by the association of drug-induced hERG blocking with an increased incidence of a fatal type of arrhythmia, named “torsades de pointes” (TdP).^{1–3} In fact, many drugs, including noncardiac drugs such as antimicrobials, neuroleptics, antipsychotics, antiarrhythmics, and antihistamines, have been withdrawn from the market or received severe restrictions on use because of hERG-related cardiotoxicity (Chart 1).^{1,2}

With repercussions in both drug discovery and clinical practice, the hERG channel has been recognized as a primary antitarget in the screening of drug candidates.^{4,5} A number of preclinical models have been developed to assess potential proarrhythmic properties.⁶ hERG liability assessment and management have become an important part of every project in the pharmaceutical industry. However, despite all of the efforts and progress obtained in the evaluation of the effects of compounds on hERG channels, QT prolongation remains a major cause of attrition during current drug development.⁷

Several issues should be recognized and investigated in the preclinical setting in order to fully assess the hERG liability of a new chemical entity. The complexity of ventricular repolarization,³ channel promiscuity, potential interactions with other ion channels, different binding modes, and modes of action^{8–10} are just a few issues that add up to the multifaceted cardiotoxicity

prediction arena. Because of the high costs and limitations of available preclinical models,¹¹ an integrated risk assessment seems desirable. Association of in silico and experimental approaches has been suggested as the cornerstone of a cost-effective and successful preclinical evaluation of the cardiotoxic risks of drug candidates.^{6,7}

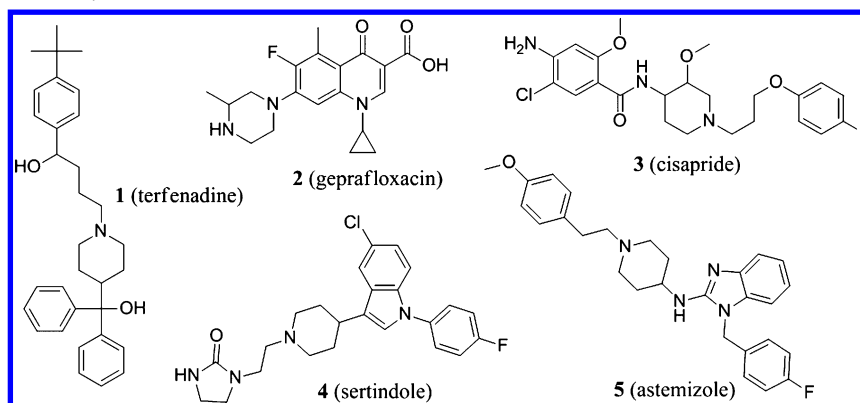
Many molecular modeling studies focused on hERG block prediction have been published, covering QSAR^{12–15} and rule-based models,¹⁶ pharmacophores,^{17–21} structure-based studies employing homology models,^{9,22} machine learning,^{23,24} and computational approaches describing the physiology of the electrical wave propagation in the heart.²⁵ Recent advances in the prediction of hERG blockage have been summarized by Wang et al.²⁶ Nonetheless, while in silico models have great potential, particularly in early drug development, only a few examples of experimentally validated models comprising publicly available data are available in the literature.^{15,17,27–31}

With the increasing need for reliable cardiotoxicity prediction tools, especially on hERG blocking and its QT prolongation potential, we designed and experimentally validated a set of complementary ligand-based pharmacophore models. This study focused on pharmacophore models because in the safety profiling field many pharmacophore models have been

Received: March 28, 2014

Published: August 22, 2014

Chart 1. Representative Structures of Drugs Withdrawn from the Market because of hERG-Related QT Interval Prolongation and Severe Risk of Fatal Arrhythmias



established and generally provide satisfactory results.^{32,33} The predictive tools developed and validated in this study were able to accurately and prospectively predict hERG blocking by novel compounds.

RESULTS AND DISCUSSION

The general workflow of this study is depicted in Figure 1. hERG blocker databases were assembled from the literature and used for generation of ligand-based hERG blocker pharmacophore models with the two software packages Discovery Studio Catalyst and LigandScout. The models were theoretically validated using literature data sets and a decoy set. Only models with high enrichment factors (EFs) and complementary virtual hits (VHs) were employed for prospective screening of compound libraries. Biological evaluation of each model was carried out by selecting 5–13 VHs for experimental validation using a patch clamp assay. All of the models except one successfully identified previously unknown hERG blockers from diverse chemical classes.

Pharmacophore Modeling. As reported before, pharmacophore generation algorithms and virtual screening (VS) protocols yield different pharmacophore models and hit lists, even if the training molecule(s) for model generation are identical.^{34,35} Remarkably, all pharmacophore programs are able to prospectively find assorted active hits, and pharmacophore algorithms can be combined together in order to increase the success of hit compound identification.^{34,35} Our goal was the achievement of a consensus set of models^{26,36} and its application in a prospective campaign rather than the direct comparison of different softwares, model generation approaches, or training data sets. Therefore, two pharmacophore modeling software packages were used for modeling and VS. As a further step aiming at high-confidence ligand-based models, only compounds with results from functional assays (e.g., patch clamp) were included during database compilation, which considerably reduced the size of the training sets. Even though on average the correlation between hERG functional and binding assays is moderate in ChEMBL,³⁰ the preparation of data sets with only high-quality data was considered a key step toward the development of reliable models.²⁶

On the one hand, a Catalyst pharmacophore model³⁷ was generated mostly on the basis of clinically used drugs. This model was designed to recognize a broad variety of hERG blockers from the literature. On the other hand, a parallel pharmacophore modeling approach³⁸ was pursued using

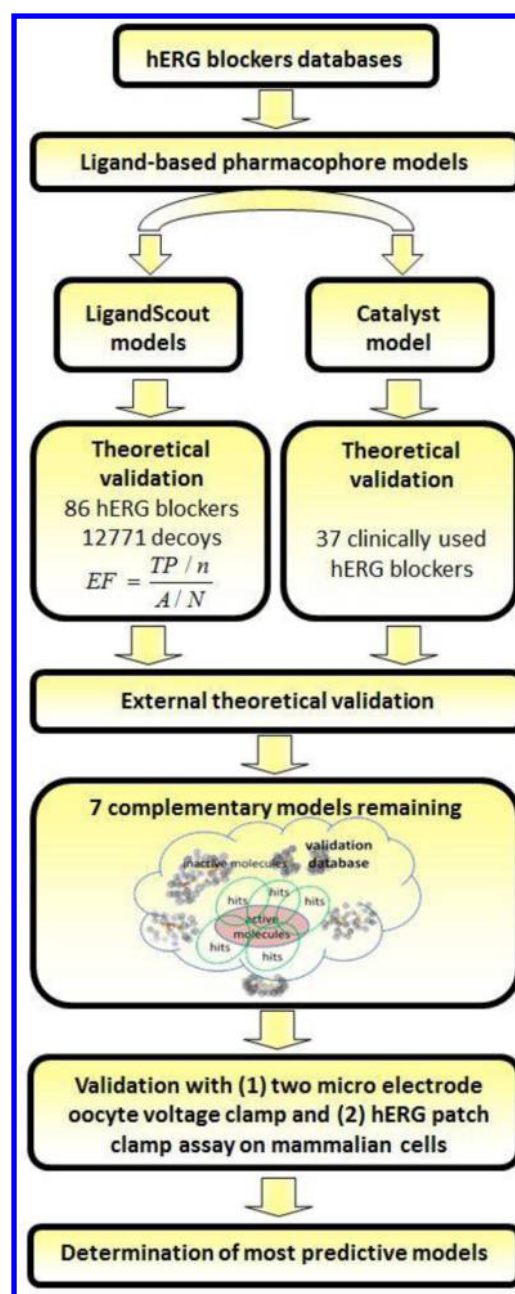
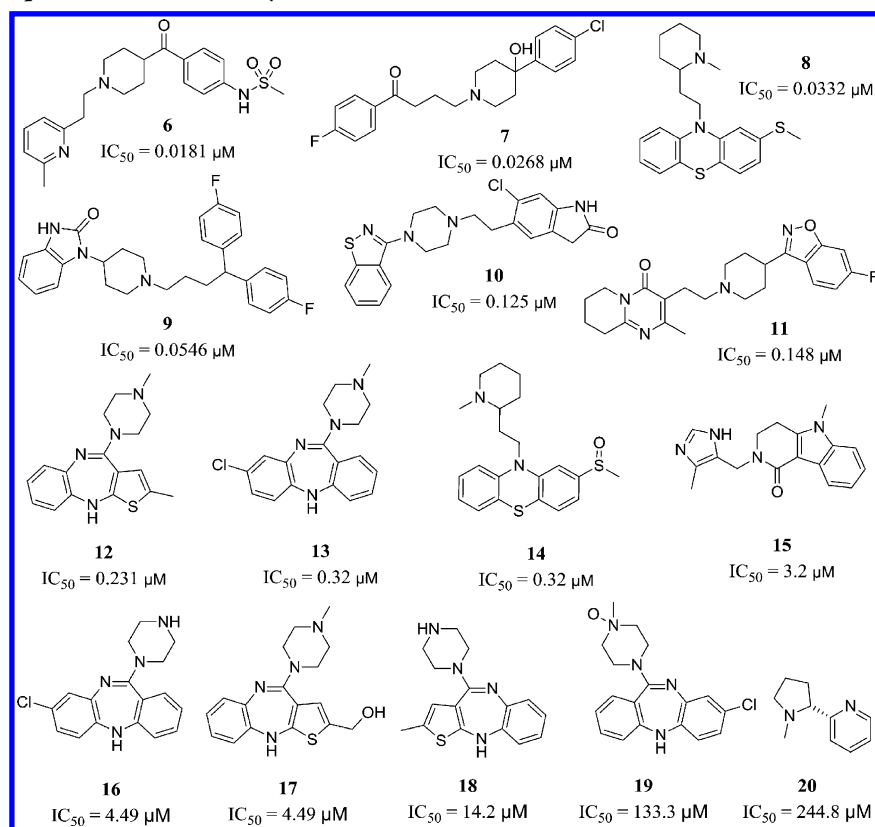


Figure 1. General workflow employed in this study.

Chart 2. Training Compounds Used for Catalyst Model Generation^a

^aCompounds 1, 3, and 4 (Chart 1) were also part of the training set.

LigandScout.³⁹ In this workflow, several pharmacophore models recognizing subsets of active compounds from the ChEMBL database and being restrictive against inactive and decoy molecules were combined. The screening model set was assembled in such a way that the majority of active compounds were correctly found while the overall number of false-positive predictions remained small.

The Catalyst pharmacophore model was based on 18 chemically diverse hERG blockers from the literature, all evaluated with the same patch clamp assay (Chart 2).¹⁵ The generated model was subsequently validated using a test set of 19 compounds compiled from previously published studies (Chart 3).^{15,40–49} Among the 10 models generated by the program, the one recognizing the most active hits from both the training and test sets was selected for further studies (Figure 2). In this theoretical validation, the Catalyst model was able to find 14 out of 18 compounds in the training set and 8 out of 19 compounds in the test set (Table 1 and Table S1 in the Supporting Information).

The pharmacophore model collection generated with LigandScout comprised six models (M1–M6), which were validated using a set of 86 highly active hERG blockers collected from the literature and a decoy set (12 771 druglike decoys supposed to be hERG-inactive). Each model was based on two training compounds (Figure 3). The refinement of each automatically generated model is described in detail in the Supporting Information.

In general, most of the models were composed of the classical pharmacophore features for hERG blockers reported by other groups: two to three hydrophobic features, some of them grouped with an aromatic ring.^{15,21,50} All of the models

but M2 incorporated one or two hydrogen-bond acceptors. Finally, four models (M3–M6) included a positively ionizable group. In comparison, the Catalyst model also fulfilled these general features with three hydrophobic/aromatic features and a positively ionizable group. Because of the unique shape of its binding site and its hydrophobic character, the hERG channel has been shown to interact with a wide range of chemical structures. In general, however, it is recognized that one or two hydrophobic groups interact with Phe656 side chains and that a basic nitrogen (protonated under biological conditions) or aromatic ring is involved in cation– π interactions with Tyr652 residues.⁵⁰ In this view, the features present in our models largely represent the classical chemical moieties present in known hERG blockers.

The performance of each model alone and also of all of the models as a single group (parallel screening) is shown in Table 2. The receiver operating characteristic (ROC) plot of the database screenings with the combined model set is given in Figure 4.

A truly valid group of pharmacophore models should be able to differentiate between active and inactive molecules and perform complementarily. The theoretical validation results showed that this gold standard was achieved for M1–M6. In the parallel screening, the models were able to cover 84.9% of truly active compounds (ranging from 8 to 30% as single models) with few false-positive hits, giving a ROC area under the curve (ROC-AUC) value of 0.91. These results indicate remarkable performance of the models in combination. In single-model appraisals, M3 showed the highest true-positive hit rate, while M2 was the most specific model. On the other hand, M4 and M3 were the most complementary models,

Chart 3. Test Compounds Used for Theoretical Validation of the Catalyst Model

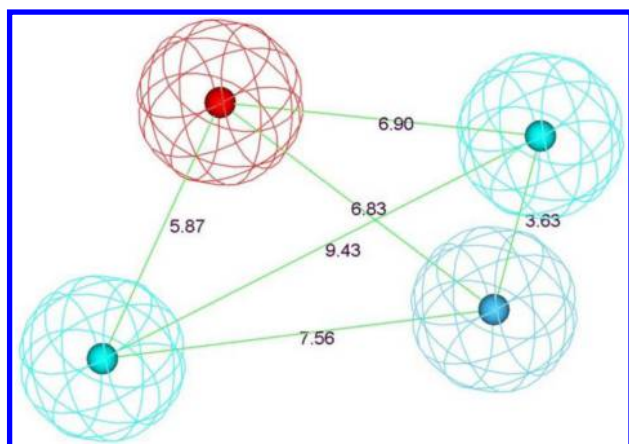
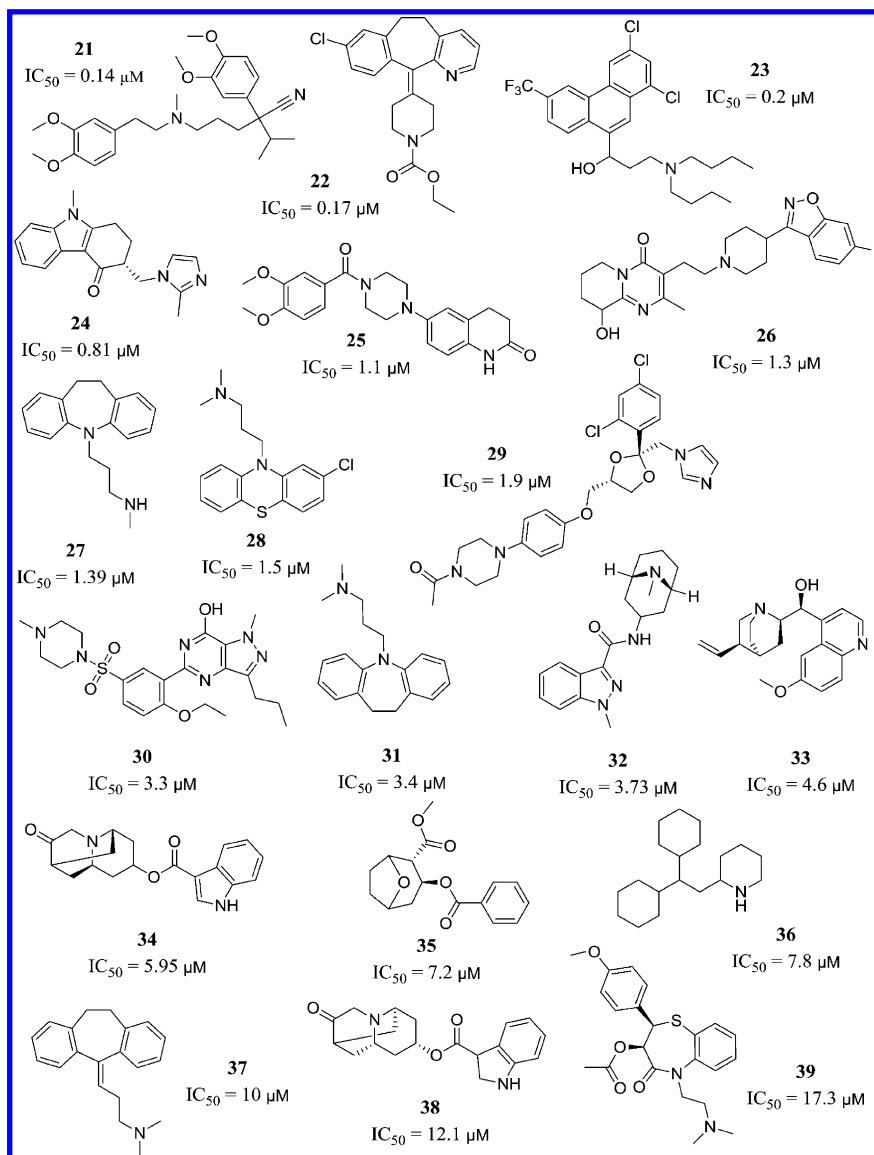


Figure 2. Catalyst pharmacophore model for hERG blockers. The indicated distances between the features are in Å. Chemical features are color-coded: positively ionizable (red); hydrophobic (cyan); aromatic hydrophobic (blue).

while M5 predicted only four unique hits. For comparison, the Catalyst model was screened against the data sets used for

models M1–M6. The model retrieved 1287 hits in the decoy set and 68 out of 86 highly active hERG blockers. Although its performance in finding active compounds was nearly comparable to that of the combined models M1–M6, it had a much higher rate of false-positive hits, as reflected by the EF of 7.5 (vs 23.1 for M1–M6).

To additionally validate the generated models and the VS strategy using an independently assembled data set, all of the active compounds discussed in an excellent review by de Bruin and co-workers⁵¹ were submitted to an activity classification (Table 3). Overall, 65% of the compounds (34 out of 52) were found by the combination of the two different software models. The Catalyst model alone was able to find 58% of the compounds, while the LigandScout models showed an inferior performance, finding only 37% of the external data set of hERG blockers. Both programs found one inactive compound, cetirizine. The hit lists presented some overlap, with 15 consensus hits, but the Catalyst and LigandScout models found 15 and four unique hits, respectively. When the analysis was restricted to potent hERG blockers with IC_{50} values of $\leq 1 \mu M$, the combination of models was able to find 89% of the highly

Table 1. Test Set Screening Results Using the Catalyst Model

compd	experimental IC ₅₀ [μ M]	found by model	ref
21	0.14	X	49
22	0.17		40
23	0.2	X	46
24	0.81		43
25	1.1		41
26	1.3	X	15
27	1.39		15
28	1.5	X	42
29	1.9		15
30	3.3	X	15
31	3.4		45
32	3.73	X	43
33	4.6	X	44
34	5.95		43
35	7.2		48
36	7.8		47
37	10		15
38	12.1		43
39	17.3	X	49

active blockers (24 out of 27). The performance of both models improved in this subset: the Catalyst model prediction

Table 2. Performance of LigandScout Models in Single and Parallel Screening against the hERG Highly Active Database and the Decoy Set

model	true-positive hits ^a	false-positive hits ^b	EF ^c	ROC-AUC ^d
M1	19 (22.09%)	20 (0.15%)	72.8	0.61
M2	13 (15.11%)	2 (0.016%)	129.6	0.58
M3	26 (30.23%)	58 (0.45%)	46.3	0.65
M4	20 (23.25%)	140 (1.10%)	18.7	0.61
M5	7 (8.13%)	2 (0.016%)	116.3	0.54
M6	24 (27.90%)	202 (1.58%)	15.9	0.63
M1–M6 ^e	73 (84.88%)	400 (3.13%)	23.1	0.91

^aVirtual hits from the highly active database (total of 86 compounds).

^bVirtual hits from the decoy set (total of 12 771 compounds). ^cThe enrichment factor (EF) measures the yield of actives proportionally to the ratio of actives in the database. The maximum theoretical EF for the data sets used in this study is 148.5. ^dReceiver operating characteristic area under the curve (ROC-AUC) values above 0.5 indicate yields better than random selection of hits (see the Experimental Section for a detailed description of model performance assessment). ^eVirtual screening was performed with all models simultaneously (parallel screening).

rate increased from 58% to 85% (23 out of 27 compounds), and the LigandScout models were able to find 44% of the highly active compounds with one additional unique hit.

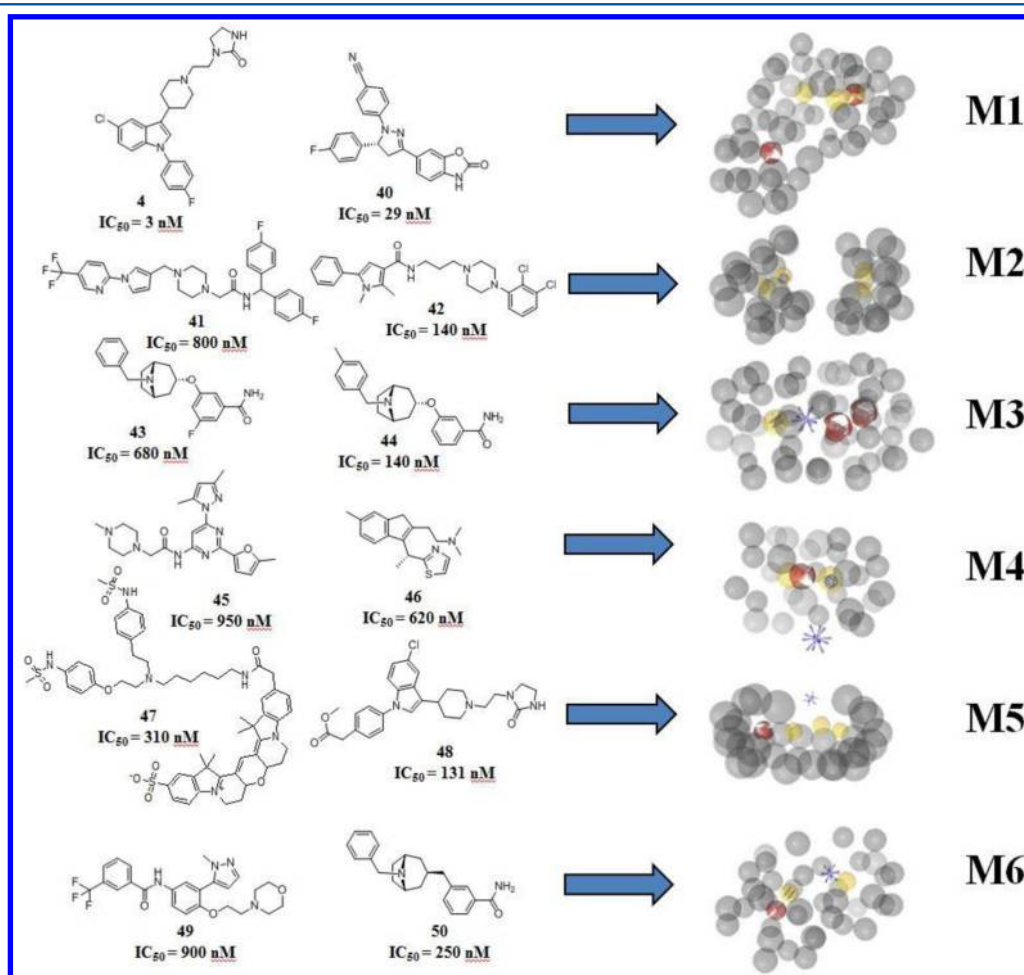


Figure 3. Training compounds and optimized ligand-based LigandScout pharmacophore models (M1–M6). Chemical features of the models are color-coded: hydrophobic (yellow); hydrogen-bond acceptor (red); aromatic rings (blue parallel rings); positively ionizable groups (blue stars); exclusion volumes (gray).

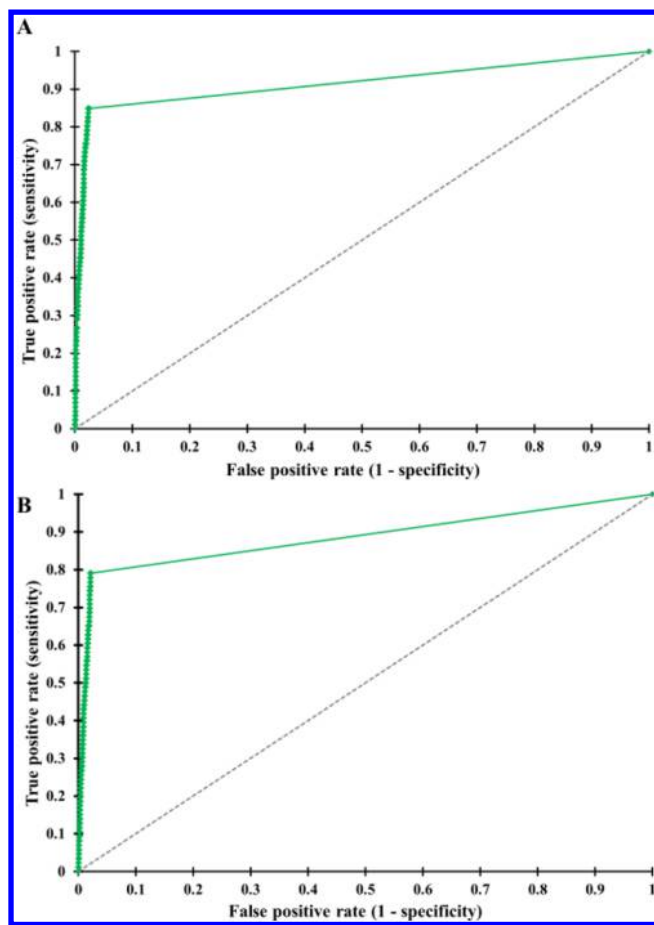


Figure 4. ROC plots for screening of the highly active database and decoy set using (A) models M1–M6 in parallel (ROC-AUC = 0.91) and (B) the Catalyst model (ROC-AUC = 0.89).

In this view, the global results obtained in the theoretical validation indicated that the main modeling objective was successfully accomplished. Complementary models were constructed, retrieving good coverage of the active compounds (average 63.50% true-positive hit rate) combined with satisfactory selectivity (average 0.55% false-positive hit rate). Therefore, we decided to use the models from both softwares for the prospective virtual screening of compound libraries in the search for putative hERG blockers to be subjected to experimental testing and for validation of the generated models.

Prospective Virtual Screening of In-House and Commercial Databases. The pharmacophore models were experimentally validated using compounds available from the in-house library of the Institute of Pharmacy at the University of Innsbruck or provided by the commercial supplier SPECS (www.specs.net). The primary goal was to obtain for each of the pharmacophore models a sufficient number of compounds predicted to be active. Initially, a prospective VS was carried out against the in-house 3D molecular database (In-house, 3986 compounds), which led to 174 and 93 VHs for LigandScout models M1–M6 and the Catalyst model, respectively (average hit rate of 3.4%). Because the hit lists presented a restricted number of chemical scaffolds and did not cover all of the models properly, the SPECS synthetic product database (SPECS SP, 202 907 compounds) and SPECS natural product database (SPECS NP, 453 compounds) were additionally screened. This endeavor retrieved more than 20 000 VHs

(average hit rate of 6.5%). The combined hit lists were clustered by structural diversity and inspected for the removal of compounds with known hERG activity. In total, 50 compounds were selected for biological evaluation with five to 13 compounds per model. As selection criteria we used the chemical diversity, high geometric fit score, consensus hits, and confirmed purity and identity (all of the tested compounds showed purities of $\geq 95\%$ as assessed by HPLC–MS). All of the structures are shown in Chart S1 in the Supporting Information.

Experimental Validation Results. In a first screening, which employed a two-microelectrode voltage clamp assay on hERG channels expressed in *Xenopus* oocytes, all of the compounds were applied at a concentration of 30 μM .⁵² Thioridazine (8), a known hERG blocker,¹⁵ was employed as a positive control. A 30% reduction in peak tail current was established as the cutoff for positive hERG blockade. This campaign identified 20 hERG blockers that showed inhibitions between 32.3 and 78.9% (Figure 5). Complete screening data, including models coverage and compound sources, are available in Table S2 in the Supporting Information.

For further in vitro characterization, a more restraining cutoff was employed. Only the 13 compounds that showed $\geq 50\%$ blocking in the preliminary screening were selected for IC_{50} determination in a patch clamp assay in HEK293 cells.^{53,54} Figure 6 shows the concentration–inhibition curves and the structures of the respective compounds. This study revealed potent concentration-dependent blocking of the hERG current by all of the compounds, with IC_{50} values ranging from 0.13 to 2.77 μM (Table 4).

Comparison of Prospective Model Performance. From the seven ligand-based pharmacophore models developed and investigated in this study, six successfully passed the theoretical and experimental validation. A final true hit rate of 40% (20 out of 50 compounds selected for biological screening) was obtained, including 10 compounds active in the submicromolar range (Table 4 and Figure 6). Regarding complementarity, 33% of the consensus hits and 50% of the single hits were active. Table 5 summarizes the prospective prediction performance.

A structure similarity search within the highly active database (Tanimoto coefficient = 0.5), using the new true hits as queries revealed that only 5 out of 13 molecules retrieved results, corroborating the scaffold hopping potential of the models (data not shown). On the other hand, although structurally diverse from the classical hERG blockers, the newly identified hERG blockers covered a part of the physicochemical drug space already populated by known hERG blockers (the chemical space analysis is shown in Figure S1 in the Supporting Information).

LigandScout models M4 and M6 as well as the Catalyst model showed superior performance, and thus, they can be considered as particularly reliable tools. The negative highlight is M2; despite its good theoretical validation, all five virtual hits tested in this study were inactive. This pharmacophore was the only model that did not include any hydrogen-bond acceptor feature, and this discrimination might be linked with the poor experimental performance. Some studies have underlined the importance of hydrogen-bond acceptor features for appropriate fitting of molecules into the hERG channel, especially for uncharged hERG blockers.^{18,36,50}

The prospectively achieved rate of true-positive hits (i.e., the success rate; Table 5) did not correlate with the enrichment rates observed in the retrospective validation (Table 2). M2, the model with the highest EF, did not find any new hERG

Table 3. Retrospective Validation Results Using the External Data Set Reported by deBruin et al.⁵¹

compd	IC ₅₀ [μ M] ^a	predicted active by Catalyst	predicted active by LigandScout	LigandScout models					
				M1	M2	M3	M4	M5	M6
astemizole (5)	0.0009	X	X	X					
cisapride (3)	0.002	X^b	X						X
terodiline	0.004								
dofetilide	0.005		X			X			
ibutilide	0.01	X	X						X
sertindole (4)	0.014	X	X	X				X	
pimozide (9)	0.015	X	X	X					
terfenadine (1)	0.02	X							
haloperidol (7)	0.027	X	X			X			
thioridazine (8)	0.033	X	X				X		
almokalant	0.05	X							
azimilide	0.1	X							
verapamil (21)	0.14	X							
risperidone (11)	0.15	X							
domperidone	0.16	X							
loratadine (22)	0.173								
aprimidine	0.23	X							
sparfloxacin	0.23								
olanzapine (12)	0.231	X							
ebastine	0.3	X	X		X				
quinidine (33)	0.3	X							
mibefradil	0.35	X	X	X					
mizolastine	0.35	X	X	X					
propafenone	0.44	X							
bepidil	0.6	X							
amiodarone	1.0	X	X				X		
tamoxifen	1.0	X							
desipramine (27)	1.39								
chlorpheniramine	1.6	X	X				X		
disopyramide	1.8	X							
ketoconazole (29)	1.9								
tedisamil	2.5								
fluoxetine	3.1	X							
imipramine (31)	3.4								
flecainide	3.91	X	X	X					X
amitriptyline (37)	4.66								
fexofenadine	5.0	X	X		X				
mefloquine	5.6		X						X
nitrendipine	10								
diltiazem (39)	10	X							
cibenzoline	23								
sematilide	25		X						X
grepafloxacin	27								
diphenhydramine	30								
clarithromycin	32.9								
erythromycin	72.2								
sotalol	74		X						X
phenytoin	100 ^c								
cetirizine	108	X	X			X			
nifedipine	275								
procainamide	310								
ciprofloxacin	966								

^aIC₅₀ values as reported in the original publications are given in the review by deBruin et al.⁵¹ ^bSince this data set was assembled completely independently from this study, some of the compounds matched ones in the training set used for model development; these are shown in bold.

^cCompounds with IC₅₀ values of >100 μ M were considered inactive.

inhibitors in the prospective screening. However, M6 and the Catalyst model, both with the lowest EFs, showed superior success rates in the experimental validation. Generally,

enrichment metrics highly depend on the data set(s) used for model validation. Therefore, the metrics calculated for only one data set may not adequately represent the actual predictive

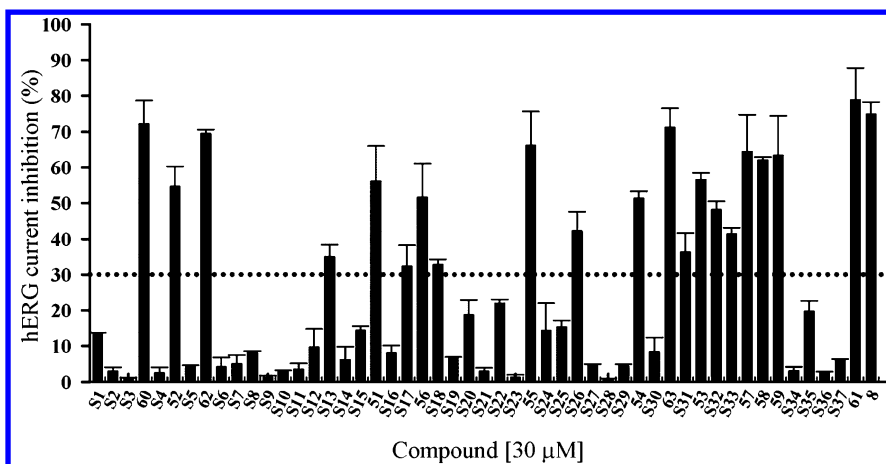


Figure 5. Inhibition of hERG current by compounds (30 μ M) in the oocyte two-microelectrode assay, given as mean \pm SE ($n = 3$ –5). Thioridazine (8) was used as a positive control.

power of a model. Thus, for a broader picture of the models' performances, additional, independently assembled, publicly available hERG data sets provided by Wang et al.²⁴ were screened (Table 6).

Similar to the previous validation screenings, all of the models performed well in terms of enriching active compounds in their hit lists. One data set, the PubChem data set, was the most challenging one of the screened databases. Some of the LigandScout models were not able to find a single active compound in this data set. However, the PubChem data were generated using a fluorescence-based hERG blocking assay in which assay interferences by chromophoric compounds cannot be excluded. Additionally, this assay clearly differs from the "gold standard" patch clamp assay used as a starting point for our modeling data sets and experimental validation of virtual hits. Also, Wang et al. retrieved their lowest general accuracy metrics with the PubChem data set.

Importantly, the LigandScout models M1–M6 and the Catalyst model did not find exclusively identical hits (Table 6). On average, 30% of the LigandScout model hits and 72% of the Catalyst model hits showed no overlap. The reasons for the diverging hits lie in the different chemical feature definitions and screening algorithms, as discussed by Spitzer et al.³⁵ and Sanders et al.³⁴

In all of the screening databases (Table 6), the poor prospective performance of M2 and the superior performances of M6 and the Catalyst model were not reflected. Anyway, it has to be considered that only up to 13 compounds were tested per model. For M2, only five hits were evaluated in vitro because of its high restrictivity. Generally, virtual databases for model validation are carefully assembled and seeded with structurally diverse, known active compounds. However, in a prospective screening, there is no preinformation available on how many active molecules from which chemical classes can be identified. It can therefore happen that a retrospectively excellently validated model does not retrieve new active hits from a prospectively used screening database.

The reported parallel screening approach aimed at a preferably complete retrieval of hERG blockers (high sensitivity) and a correct classification of inactive compounds (high specificity). The latter was achieved with very low false-positive hit rates in all the investigated databases. The specificity was even superior to the machine learning models reported by Wang et al. The sensitivity, however, could still be improved to identify also smaller and

chemically more diverse true-positive hits. For example, one of the (aromatic) hydrophobic features from the Catalyst model could be set as optional. This small change in the model would immediately considerably improve the true-positive hit rate by, for example, enabling highly active compounds like terodiline to map all of the required features. However, at the same time, the specificity of the model and, in turn, its EFs would decrease. This would lead to an unacceptable amount of virtual hits (average 30% of database entries), hindering the focus on the most probable hERG blockers.

Regarding the relevance of the novel hERG blockers found in this study, among the hits are neuroleptic drugs (azaperone, 51), intermediary products in organic chemistry (phenodanisyl, 52), local anesthetics (cinchocaine, 54), and natural products. Even though the association between cardiotoxicity and in vitro hERG blocking is sometimes misleading, some authors already suggest "cardiac safety margins" of at least 30-fold between the ED₅₀ of a drug and its IC₅₀ on the hERG channel. An extensive evaluation of 100 drugs done in 2003 by Redfern et al.⁴ supports the safety margin of 30-fold for the treatment of serious illnesses. Furthermore, they suggest a safety margin of >100-fold for the treatment of less serious illnesses, while a safety margin of >10-fold may be acceptable for a medication for life-threatening diseases.

Voacangine (53), which showed an IC₅₀ value of 0.30 ± 0.08 , is an iboga alkaloid found in the root bark of *Voacanga africana* and other species.⁵⁵ This compound serves as a precursor for the semisynthesis of ibogaine, a not-licensed antiaddictive iboga alkaloid. The potent hERG blocking effect of ibogaine has been published recently,^{55,56} after we selected its close analogue, voacangine, from our virtual hit list as a hERG blocking candidate for biological testing.

Although the predictive power of most of the reported models was high, the use of these models for predictive screening studies needs to be performed with caution. The theoretical model validation already showed that the models could not correctly identify 100% of the active compounds from the literature. As in many virtual screening approaches, model optimization here is a balancing act between sensitivity and specificity.⁵⁷ For the hERGscreen project, it was more important to find active compounds with comparably low experimental efforts. Therefore, the more restrictive models were favored.

However, when screening for potentially toxic effects, it is desirable to detect all relevant compounds. The models can

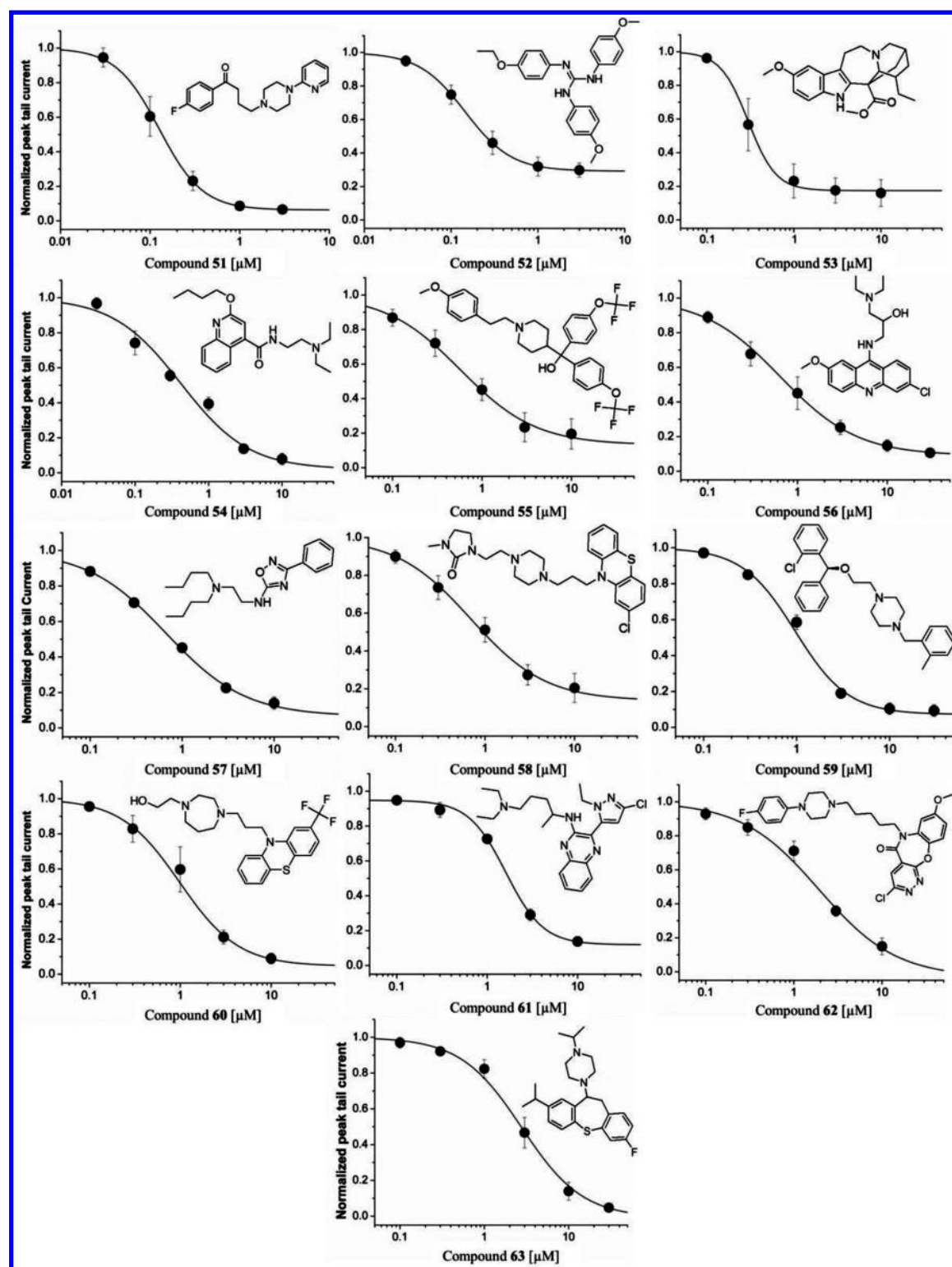


Figure 6. Concentration–response curves of hERG current inhibition by compounds in the HEK293 cells patch clamp assay ($n = 3–5$). Only compounds that showed $\geq 50\%$ blocking in the preliminary screening were selected for this further validation step.

therefore mainly be used to prioritize compounds likely to be active hERG blockers, since a compound not fitting into the models may still be active. The reported model collection presented in this study will be even more useful when complemented by other virtual classification tools. For instance, models developed by means of machine learning methods, which employ inactive compounds in large numbers, are likely

to cover a broader chemical property space and represent good candidates for balancing our approach.^{23,24,26,58}

CONCLUSION

Several pharmacophore models have been developed in this study using two different software tools. On the basis of a theoretical validation, seven models have been qualified with

Table 4. Inhibitory Activities of Selected Compounds in HEK 293 Cells Expressing hERG Channels in the Planar Patch Clamp Assay

compd	IC ₅₀ [μ M] ^a	prediction ^b
51	0.13 \pm 0.02	M3
52	0.15 \pm 0.03	M1
53	0.30 \pm 0.08	M6
54	0.42 \pm 0.07	M6
55	0.58 \pm 0.24	M5
56	0.64 \pm 0.14	M4, Catalyst
57	0.67 \pm 0.10	Catalyst
58	0.70 \pm 0.28	M4, Catalyst
59	0.96 \pm 0.09	Catalyst
60	0.99 \pm 0.22	M1, M6
61	1.61 \pm 0.14	M4, Catalyst
62	1.92 \pm 0.69	M1, Catalyst
63	2.77 \pm 0.61	M6

^amean IC₅₀ \pm SE ($n = 3-5$). ^bVirtual hit of the depicted model(s) in the prospective virtual screening.

Table 5. Individual Model Performance Evaluation Based on the Experimental Results

model	tested compds ^a	active compds ^b	success rate
M1	8	3	37.5%
M2	5	0	00.0%
M3	6	2	33.3%
M4	11	5	45.5%
M5	6	2	33.3%
M6	9	6	66.7%
Catalyst	13	8	61.5%

^aNumber of predicted compounds tested, considering consensus hits.

^bNumber of compounds that reached at least 30% reduction of hERG peak tail current in the patch clamp assay in *Xenopus* oocytes.

high predictive power. Experimental validation further attested the Catalyst model and five of the six generated LigandScout models for application in a preclinical stage to identify putative hERG channel blockers from large data sets.

The experimental confirmation that the models developed in this study can accurately predict hERG blocking by previously unknown compounds of natural origin is of special interest. These models (the Catalyst model together with a parallel screening in LigandScout with all models excluding M2) are currently implemented as prediction tools in an ongoing EU project (hERGscreen, 295174, www.uibk.ac.at/pharmazie/pharmakognosie/hergscreen), where we aim at target-oriented identification and isolation of hERG channel blockers from commonly consumed botanicals. The repercussions of hERG blockage for drug candidates and its awareness are reflected in the guideline for the nonclinical strategy to unmask the QT-prolonging potential by human pharmaceuticals published by the International Conference on Harmonisation (ICH) in 2005 (ICH S7B Guideline).⁵ This regulation, however, has never been systematically applied on botanicals. As natural products, such as dietary supplements, spices, and herbal medicinal products, continue to increase in popularity, there is an urgent need for studies aimed at critically assessment of their potential cardiotoxic risks. Highly potent hERG blockers present in these products, even in small amounts, can threaten the “cardiac safety margins” proposed by some authors.⁴ The EU project’s efforts accordingly aim at determining, identifying, understanding,

Table 6. Screening of the LigandScout Models M1–M6 and the Catalyst Model against Four External Data Sets Provided by Wang et al.²⁴

Wang data set (actives/decoys)	M1 (%EF _{max})	M2 (%EF _{max})	M3 (%EF _{max})	M4 (%EF _{max})	M5 (%EF _{max})	M6 (%EF _{max})	M1–M6 (%EF _{max})	Catalyst (%EF _{max})	common hits of M1–M6 and Catalyst
training (303/300)	9/4 (69.2)	6/0 (100)	34/5 (87.2)	17/2 (89.5)	5/1 (83.3)	8/4 (66.7)	71/15 (82.6)	141/36 (79.7)	42
test (61/59)	6/0 (100)	1/0 (100)	5/0 (100)	2/0 (100)	0/0 (—)	2/0 (100)	13/0 (100)	33/8 (80.5)	10
WOMBAT (55/11)	0/0 (—)	0/0 (—)	7/1 (87.5)	3/1 (40.9)	2/0 (100)	2/0 (100)	12/2 (85.7)	31/0 (100)	8
Pubchem (250/1693)	0/1 (0)	2/2 (50)	1/7 (12.5)	16/13 (55.2)	0/2 (0)	0/13 (0)	19/33 (36.5)	61/98 (38.4)	15

and ultimately reducing the cardiotoxic safety liabilities of frequently used botanicals. The pharmacophore models generated and validated in this study now offer the possibility to mine large natural product databases to prioritize botanicals with putative hERG blocking activities to be phytochemically investigated in detail and subjected to focused biological testing.

■ EXPERIMENTAL SECTION

Hardware and Software. In silico studies were carried out on workstations running Windows Vista, Windows 7, and/or Linux CentOS 5. Pharmacophore modeling and VS experiments were performed using LigandScout 3.03b (Inte:Ligand, Vienna, Austria),³⁹ Catalyst 4.7, and Discovery Studio 3.0 (Accelrys Inc., San Diego, CA, USA, 2001–2013). Structural conformational analyses were performed in OMEGA version 2.3.3,^{59–61} as incorporated in LigandScout, and Catalyst 4.7 or Discovery Studio 3.0. Structural clustering was calculated using Discovery Studio 3.0. Structural drawing was performed in ChemBioDraw Ultra 12 (CambridgeSoft Corp., Cambridge, MA, USA).

Database Compilation and Preparation. *LigandScout Models.* For pharmacophore model development in LigandScout, databases of published compounds with known hERG blocking activities were assembled. As the data source, the ChEMBL platform⁶² (version 12) was used. All of the compounds with annotated hERG activity data were analyzed. Only hERG blocking activities determined using patch clamp techniques⁶³ were kept. Six additional compounds from the recent literature^{64–68} were added to the data set, resulting in a database of 609 entries. Each molecular structure and activity annotation was checked for correctness in the original literature. This data set was split into three sections: (i) highly active hERG blockers with $IC_{50} \leq 1 \mu M$ ($n = 141$), (ii) active compounds with IC_{50} values between 1 and $100 \mu M$ ($n = 448$), and (iii) inactive molecules with $IC_{50} > 100 \mu M$ ($n = 20$). In order to remove redundant information on structurally similar compounds from the same activity class, each set was clustered by molecular diversity using FCFP6 fingerprints available in Discovery Studio. Further on, by visual inspection of the clusters, only the most diverse molecules were kept. The final highly active set comprised 86 compounds, the active set 206 structures, and the inactive set 19 molecules. These data sets were converted into 3D multiconformational databases using OMEGA as incorporated in LigandScout. The BEST settings were used, calculating up to 400 conformers per molecule.

Catalyst Data Set. For model generation and validation, a literature data set comprising 37 drugs was assembled, with a focus on clinically used hERG blockers. The compounds were generated with the molecule builder in Catalyst 4.7 and submitted to conformational analysis using the BEST settings with a maximum number of 250 conformers per molecule and an energy range of a maximum of 20 kcal/mol above the calculated energy minimum.

Decoy Set. For theoretical validation of LigandScout models, a previously reported decoy set was used.⁶⁹ Decoys are molecules that most likely do not show any binding affinity to the target but whose bioactivity has not yet been tested. 3D conformations of the structures were calculated using OMEGA and incorporated into LigandScout using the FAST configuration; 100 conformations were calculated for each structure. The result was an optimized 3D multiconformational screening database with 12 771 molecules.

External Data Set. For the retrospective theoretical validation of all models, an external database comprising 52 known hERG blockers was compiled. This data set was previously published by de Bruin and co-workers.⁵¹ For each compound, a maximum of 100 conformers were computed with BEST settings using OMEGA and incorporated into LigandScout or Discovery Studio.

SPECS and In-House Databases. Both synthetic (SPECS SP) and natural product (SPECS NP) collections were downloaded from the company's Web site (Nov 2012; www.specs.net). The structures from compounds available in-house were drawn using ChemBioDraw. 3D multiconformational screening databases were created using OMEGA and incorporated into LigandScout or Discovery Studio. For each molecule entry, a maximum of 100 conformers was computed with BEST settings, except for SPECS NP, in which 400 conformers were computed. The final SPECS SP, SPECS NP, and In-house databases consisted of 202 907, 453, and 3986 unique entries, respectively.

Generation of Ligand-Based 3D Pharmacophore Models. *LigandScout Models.* The highly active ChEMBL database (86 compounds) was loaded into the espresso module of LigandScout set with the default configuration and exclusion volume coating. This module employs the molecular alignment algorithm for shared feature pharmacophore model generation.^{70,71} The initial goal was to achieve a set of complementary models. For that, two unique molecules were selected as templates for the calculation of each of the six pharmacophore models (M1–M6) developed in this study (detailed information is given in the Supporting Information).

Catalyst Model. The 18 training set compounds were the basis for calculating a HypoGen pharmacophore model⁷² within Catalyst 4.7. All 10 calculated models were used to screen the training and test set compounds (Charts 2 and 3). The model that found the highest number of active hERG blockers from both data sets was selected for prospective virtual screening studies.

Theoretical Validation. Two approaches were taken for the assessment of theoretical performance. Models M1–M6 were screened against the highly active ChEMBL database and the decoy database. For VS, the “pharmacophore-fit” scoring function in LigandScout was employed, with the maximum number of omitted features set to zero. Two performance descriptors were used to evaluate the overall performance of the models. The enrichment factor (EF), which measures the yield of actives proportionally to the ratio of actives in the database, was calculated using the equation⁷¹

$$EF = \frac{(TP/n)}{(A/N)}$$

where TP is the number of truly active compounds found, n is the number of hits from the database search, A is the number of actives in the database, and N is the total number of database molecules. The second approach was the construction of a ROC curve and the calculation of the ROC-AUC. The ROC curve combines the sensitivity (Se) and specificity (Sp) into a graph that displays the increase in false positives that results with increased true positives. The Se and Sp are defined according to the equations⁷¹

$$Se = \frac{TP}{TP + FN}$$

and

$$Sp = \frac{TN}{TN + FP}$$

where TP is the number of retrieved true positives, TN is the number of rejected truly negative compounds, FP is the number of retrieved false-positive compounds, and FN is the number of false-negative compounds. A review of pharmacophore performance descriptors has been provided by Seidel et al.⁷¹ For the Catalyst model evaluation, the initial database was divided into training and test sets. Both sets were virtually screened in Discovery Studio using the best flexible search algorithm, and fit calculations were performed using the “best fit” mode.

As a final step, a retrospective validation of all of the models was performed using a previously published external data set of known hERG blockers.⁵¹ Virtual screening was carried out as described above.

Prospective Virtual Screening and Selection of Test Compounds. The SPECS SP, SPECS NP, and In-house databases were screened using the same settings as for the theoretical validation. After clustering and visual inspection of VHs covering all pharmacophore models, compounds were selected for biological testing on the basis of chemical diversity. Compounds were either obtained from in-house libraries or purchased from SPECS. Stock solutions (3–10 mM) were prepared in dimethyl sulfoxide (DMSO) and stored at –20 °C until further use. The identity and purity of compounds were determined by means of thin-layer chromatography (TLC), high-performance liquid chromatography–mass spectrometry (HPLC–MS), and differential scanning calorimetry (DSC) analyses. All of the biologically tested compounds showed purities of ≥95%.

Experimental Validation. Initial hERG Block Screening in Oocytes. Preparation of stage V–VI oocytes from *Xenopus laevis* (NASCO, Fort Atkinson, WI, USA), synthesis of capped-runoff complementary RNA (cRNA) transcripts from linearized complementary DNA (cDNA) templates, and injection of cRNA were performed as described previously.⁷³ hERG cDNAs were kindly provided by Dr. Sanguinetti (University of Utah, Salt Lake City, UT, USA). Currents through hERG channels were studied 1–3 days after cRNA injection using a two-microelectrode voltage clamp technique with a Turbo TEC-03X amplifier (npi electronic GmbH, Tamm, Germany). The extracellular recording solution contained 96 mM NaCl, 2 mM KCl, 1 mM MgCl₂, 5 mM HEPES, and 1.8 mM CaCl₂ (pH 7.5). The voltage-recording and current-injecting microelectrodes were filled with 3 M KCl and had resistances between 0.5 and 2 MΩ. Endogenous currents did not exceed 0.2 μA. Currents of >3 μA were discarded to minimize voltage clamp errors. A precondition for all measurements was the achievement of stable peak current amplitudes over periods of 10 min after an initial run-up period. Stocks were diluted in extracellular solution on the day of each experiment, and the maximal DMSO concentration (1%) did not affect the hERG currents. All compounds (30 μM) were applied by means of a fast perfusion system (ScreeningTool, npi electronic GmbH).⁵² Thioridazine hydrochloride (Sigma-Aldrich GmbH, Vienna, Austria) was used as a positive control. The pClamp software package version 10.1 (Molecular Devices, Sunnyvale, CA, USA) was used for data acquisition.

Cell Culture. Human embryonic kidney (HEK 293) cells stably expressing hERG (a kind gift from Dr. Craig January, University of Wisconsin, Madison, WI, USA) were cultured in

minimum essential medium (MEM) (Life Technologies, Vienna, Austria) containing 10% fetal bovine serum (Life Technologies), 400 μg/mL G418 (Eubio, Vienna, Austria), and 100 units/mL penicillin–streptomycin (Sigma-Aldrich) at 37 °C in an atmosphere of 5% CO₂ and 95% air. Before electrophysiological measurements, cells were harvested from their culture flasks using TrypLE Express (Life Technologies) and centrifuged at 1000 rpm for 4 min. The pellet was then resuspended in the extracellular solution and directly used for electrophysiological recording.

Whole-Cell Planar Patch Clamp. Currents through hERG channels stably expressed in HEK 293 cells were studied within 8 h of harvest in the whole-cell configuration of the planar patch clamp technique (NPC-16 Patchliner, Nanion Technologies GmbH, Munich, Germany), using an EPC 10 patch clamp amplifier (HEKA Elektronik Dr. Schulze GmbH, Lambrecht/Pfalz, Germany).^{53,54} Currents were low-pass-filtered at 10 kHz using the internal Bessel filter and sampled at 25 kHz. The extracellular solution contained 140 mM NaCl, 4 mM KCl, 2 mM CaCl₂, 1 mM MgCl₂, 5 mM D-glucose, and 10 mM HEPES (pH 7.4) (Sigma-Aldrich). The intracellular solution contained 50 mM KCl, 10 mM NaCl, 60 mM KF, 20 mM EGTA, and 10 mM HEPES (pH 7.2) (Sigma-Aldrich). Compound solutions were applied by means of the automated NPC-16 Patchliner planar patch clamp platform. PatchMaster software version 2.65 (HEKA Elektronik Dr. Schulze GmbH) was used for data acquisition.

Voltage Protocol. For the electrophysiological studies with both systems, stable peak current amplitudes over 10 min after an initial run-up phase constituted a precondition for the measurements. The voltage protocol was designed to simulate voltage changes during a cardiac action potential with a 300 ms depolarization to +20 mV (analogous to a plateau phase), a repolarization for 300 ms to –40 mV to induce a tail current (–50 mV for whole-cell patch clamp), and a final step to the holding potential (–100 mV). The +20 mV depolarization rapidly inactivates hERG channels, thereby limiting the amount of outward current. During the repolarization to –40/–50 mV, the previously activated channels open as a result of rapid recovery from inactivation. The decrease in the resulting tail current amplitude was taken as a measure of block development during a pulse train.

Data Analysis. Origin software version 7.0 (OriginLab Corp., Northampton, MA, USA) was employed for data analysis and curve fitting. The cumulative concentration–inhibition curves were fitted using the Hill equation:

$$\frac{I_{\text{hERG,drug}}}{I_{\text{hERG,control}}} = \frac{100 - A}{1 + \left(\frac{C}{IC_{50}}\right)^{n_H}} + A$$

in which IC₅₀ is the concentration at which hERG inhibition is half-maximal, C is the applied drug concentration, A is the fraction of hERG current that is not blocked, and n_H is the Hill coefficient.⁷⁴ Data are presented as mean ± standard error (SE) for at least three oocytes from two different batches or for three independent measurements with HEK 293 cells.

■ ASSOCIATED CONTENT

Supporting Information

A chart of all 50 compounds selected for biological testing; fit scores and detailed hERG screening data; additional information on the development of models M1–M6; training set screening

results for the Catalyst model; 3D scatter plots depicting the drug chemical property space of novel hERG blockers; and full experimental procedures for the syntheses of compounds **62**, **S3**, **S4**, **S5**, **S12**, **S24**, **S36**, and **S37**. This material is available free of charge via the Internet at <http://pubs.acs.org>.

AUTHOR INFORMATION

Corresponding Authors

*Phone: 0043 512 507 58407. Fax: 0043 512 507 58499.
E-mail: Judith.Rollinger@uibk.ac.at.

*Phone: 0043 512 507 58253. Fax: 0043 512 507 58299.
E-mail: Daniela.Schuster@uibk.ac.at.

Funding

This research was supported by a Marie Curie International Research Staff Exchange Scheme Fellowship within the Seventh European Community Framework Programme (hERGscreen, 295174). D.S. thanks the University of Innsbruck for her position in the Erika Cremer Habilitation Program and for a Young Talents Grant. This study was supported by FWF Grant P22395 to S.H. Financial support by the graduate school program MolTag (Austrian Science Fund FWF, grant W1231) to P.S. is gratefully acknowledged.

Notes

The authors declare no competing financial interest.

ACKNOWLEDGMENTS

We thank Prof. Ronald Gust, Dr. Gerhard Pürstinger, and Prof. Ulrich Griesser for providing the in-house compounds for biological testing, Stefan M. Noha and Teresa Kaserer for technical assistance, Philipp Schuster for help with manuscript preparation, and J. Theiner for carrying out elemental analyses.

ABBREVIATIONS

AR, aromatic ring feature; AUC, area under the curve; DSC, differential scanning calorimetry; EF, enrichment factor; EXVOLs, exclusion volume spheres; HBA, hydrogen-bond acceptor; HBD, hydrogen-bond donor; HEK 293, human embryonic kidney cells; HPFs, hydrophobic features; MEM, minimum essential medium; PIF, positive ionizable feature; ROC, receiver operating characteristic; SPECS NP, SPECS natural product database; SPECS SP, SPECS synthetic compound database; TdP, torsades de pointes; VH, virtual hit; VS, virtual screening.

REFERENCES

- (1) Yap, Y. G.; Camm, A. J. Drug induced QT prolongation and torsades de pointes. *Heart* **2003**, *89*, 1363–1372.
- (2) Sanguinetti, M. C.; Tristani-Firouzi, M. hERG potassium channels and cardiac arrhythmia. *Nature* **2006**, *440*, 463–469.
- (3) Vandenberg, J. I.; Perry, M. D.; Perrin, M. J.; Mann, S. A.; Ke, Y.; Hill, A. P. hERG K⁺ channels: Structure, function, and clinical significance. *Physiol. Rev.* **2012**, *92*, 1393–1478.
- (4) Redfern, W. S.; Carlsson, L.; Davis, A. S.; Lynch, W. G.; MacKenzie, I.; Palethorpe, S.; Siegl, P. K.; Strang, I.; Sullivan, A. T.; Wallis, R.; Camm, A. J.; Hammond, T. G. Relationships between preclinical cardiac electrophysiology, clinical QT interval prolongation and torsade de pointes for a broad range of drugs: Evidence for a provisional safety margin in drug development. *Cardiovasc. Res.* **2003**, *58*, 32–45.
- (5) *Guidance on S7B Nonclinical Evaluation of the Potential for Delayed Ventricular Repolarization (QT Interval Prolongation) by Human Pharmaceuticals*; International Conference on Harmonisation: Geneva, 2005; pp 1–9

- (6) Raschi, E.; Ceccarini, L.; De Ponti, F.; Recanatini, M. hERG-related drug toxicity and models for predicting hERG liability and QT prolongation. *Expert Opin. Drug Metab. Toxicol.* **2009**, *5*, 1005–1021.
- (7) Chi, K. R. Revolution dawning in cardiotoxicity testing. *Nat. Rev. Drug Discovery* **2013**, *12*, 565–567.
- (8) Dennis, A.; Wang, L.; Wan, X.; Ficker, E. hERG channel trafficking: Novel targets in drug-induced long QT syndrome. *Biochem. Soc. Trans.* **2007**, *35*, 1060–1063.
- (9) Durdagi, S.; Deshpande, S.; Duff, H. J.; Noskov, S. Y. Modeling of open, closed, and open-inactivated states of the hERG1 channel: Structural mechanisms of the state-dependent drug binding. *J. Chem. Inf. Model.* **2012**, *52*, 2760–2774.
- (10) Vilums, M.; Overman, J.; Klaasse, E.; Scheel, O.; Brussee, J.; Ijzerman, A. P. Understanding of molecular substructures that contribute to hERG K⁺ channel blockade: Synthesis and biological evaluation of E-4031 analogues. *ChemMedChem* **2012**, *7*, 107–113.
- (11) Lawrence, C. L.; Pollard, C. E.; Hammond, T. G.; Valentin, J. P. In vitro models of proarrhythmia. *Br. J. Pharmacol.* **2008**, *154*, 1516–1522.
- (12) Tan, Y.; Chen, Y.; You, Q.; Sun, H.; Li, M. Predicting the potency of hERG K⁺ channel inhibition by combining 3D-QSAR pharmacophore and 2D-QSAR models. *J. Mol. Model.* **2012**, *18*, 1023–1036.
- (13) Su, B. H.; Shen, M. Y.; Esposito, E. X.; Hopfinger, A. J.; Tseng, Y. J. In silico binary classification QSAR models based on 4D-fingerprints and MOE descriptors for prediction of hERG blockage. *J. Chem. Inf. Model.* **2010**, *50*, 1304–1318.
- (14) Polak, S.; Wiśniowska, B.; Ahmadi, M.; Mendyk, A. Prediction of the hERG potassium channel inhibition potential with use of artificial neural networks. *Appl. Soft Comput.* **2011**, *11*, 2611–2617.
- (15) Ekins, S.; Crumb, W. J.; Sarazan, R. D.; Wikel, J. H.; Wrighton, S. A. Three-dimensional quantitative structure–activity relationship for inhibition of human ether-a-go-go-related gene potassium channel. *J. Pharmacol. Exp. Ther.* **2002**, *301*, 427–434.
- (16) Rayan, A.; Falah, M.; Raiyn, J.; Da'adoosh, B.; Kadan, S.; Zaid, H.; Goldblum, A. Indexing molecules for their hERG liability. *Eur. J. Med. Chem.* **2013**, *65*, 304–314.
- (17) Cavalli, A.; Poluzzi, E.; De Ponti, F.; Recanatini, M. Toward a Pharmacophore for Drugs Inducing the Long QT Syndrome: Insights from a CoMFA Study of HERG K⁺ Channel Blockers. *J. Med. Chem.* **2002**, *45*, 3844–3853.
- (18) Durdagi, S.; Duff, H. J.; Noskov, S. Y. Combined receptor and ligand-based approach to the universal pharmacophore model development for studies of drug blockade to the hERG1 pore domain. *J. Chem. Inf. Model.* **2011**, *51*, 463–474.
- (19) Johnson, S. R.; Yue, H.; Conder, M. L.; Shi, H.; Doweiko, A. M.; Lloyd, J.; Levesque, P. Estimation of hERG inhibition of drug candidates using multivariate property and pharmacophore SAR. *Bioorg. Med. Chem.* **2007**, *15*, 6182–6192.
- (20) Leong, M. K. A novel approach using pharmacophore ensemble/support vector machine (PhE/SVM) for prediction of hERG liability. *Chem. Res. Toxicol.* **2007**, *20*, 217–226.
- (21) Yamakawa, Y.; Furutani, K.; Inanobe, A.; Ohno, Y.; Kurachi, Y. Pharmacophore modeling for hERG channel facilitation. *Biochem. Biophys. Res. Commun.* **2012**, *418*, 161–166.
- (22) Coi, A.; Bianucci, A. M. Combining structure- and ligand-based approaches for studies of interactions between different conformations of the hERG K⁺ channel pore and known ligands. *J. Mol. Graphics Modell.* **2013**, *46*, 93–104.
- (23) Wang, M.; Yang, X.-G.; Xue, Y. Identifying hERG potassium channel inhibitors by machine learning methods. *QSAR Comb. Sci.* **2008**, *27*, 1028–1035.
- (24) Wang, S.; Li, Y.; Wang, J.; Chen, L.; Zhang, L.; Yu, H.; Hou, T. ADMET evaluation in drug discovery. 12. Development of binary classification models for prediction of hERG potassium channel blockage. *Mol. Pharmaceutics* **2012**, *9*, 996–1010.
- (25) Zemzemi, N.; Bernabeu, M. O.; Saiz, J.; Cooper, J.; Pathmanathan, P.; Mirams, G. R.; Pitt-Francis, J.; Rodriguez, B. Computational assessment of drug-induced effects on the electrocardiogram: From ion

channel to body surface potentials. *Br. J. Pharmacol.* **2013**, *168*, 718–733.

(26) Wang, S.; Li, Y.; Xu, L.; Li, D.; Hou, T. Recent developments in computational prediction of hERG blockage. *Curr. Top. Med. Chem.* **2013**, *13*, 1317–1326.

(27) Broccatelli, F.; Mannhold, R.; Moriconi, A.; Giuli, S.; Carosati, E. QSAR modeling and data mining link Torsades de Pointes risk to the interplay of extent of metabolism, active transport, and hERG liability. *Mol. Pharmaceutics* **2012**, *9*, 2290–2301.

(28) Doddareddy, M. R.; Klaasse, E. C.; Shagufta, I.; Jzerman, A. P.; Bender, A. Prospective validation of a comprehensive in silico hERG model and its applications to commercial compound and drug databases. *ChemMedChem* **2010**, *5*, 716–729.

(29) Beattie, K. A.; Luscombe, C.; Williams, G.; Munoz-Muriedas, J.; Gavaghan, D. J.; Cui, Y.; Mirams, G. R. Evaluation of an in silico cardiac safety assay: Using ion channel screening data to predict QT interval changes in the rabbit ventricular wedge. *J. Pharmacol. Toxicol. Methods* **2013**, *68*, 88–96.

(30) Czodrowski, P. hERG me out. *J. Chem. Inf. Model.* **2013**, *53*, 2240–2251.

(31) Gavaghan, C. L.; Arnby, C. H.; Blomberg, N.; Strandlund, G.; Boyer, S. Development, interpretation and temporal evaluation of a global QSAR of hERG electrophysiology screening data. *J. Comput.-Aided Mol. Des.* **2007**, *21*, 189–206.

(32) Ekins, S.; Mestres, J.; Testa, B. In silico pharmacology for drug discovery: Applications to targets and beyond. *Br. J. Pharmacol.* **2007**, *152*, 21–37.

(33) Schuster, D. 3D pharmacophores as tools for activity profiling. *Drug Discovery Today: Technol.* **2010**, *7*, e205–e211.

(34) Sanders, M. P.; Barbosa, A. J.; Zarzycka, B.; Nicolaes, G. A.; Klomp, J. P.; de Vlieg, J.; Del Rio, A. Comparative analysis of pharmacophore screening tools. *J. Chem. Inf. Model.* **2012**, *52*, 1607–1620.

(35) Spitzer, G. M.; Heiss, M.; Mangold, M.; Markt, P.; Kirchmair, J.; Wolber, G.; Liedl, K. R. One concept, three implementations of 3D pharmacophore-based virtual screening: Distinct coverage of chemical search space. *J. Chem. Inf. Model.* **2010**, *50*, 1241–1247.

(36) Du-Cuny, L.; Chen, L.; Zhang, S. A critical assessment of combined ligand- and structure-based approaches to hERG channel blocker modeling. *J. Chem. Inf. Model.* **2011**, *51*, 2948–2960.

(37) *Catalyst Software Package*, version 4.7; Accelrys Software Inc.: San Diego, CA, 2003.

(38) Schuster, D.; Waltenberger, B.; Kirchmair, J.; Distinto, S.; Markt, P.; Stuppner, H.; Rollinger, J. M.; Wolber, G. Predicting cyclooxygenase inhibition by three-dimensional pharmacophoric profiling. Part I: Model generation, validation and applicability in ethnopharmacology. *Mol. Inf.* **2010**, *29*, 75–86.

(39) Wolber, G.; Langer, T. LigandScout: 3-D pharmacophores derived from protein-bound ligands and their use as virtual screening filters. *J. Chem. Inf. Model.* **2005**, *45*, 160–169.

(40) Crumb, W. J., Jr. Loratadine blockade of K⁺ channels in human heart: Comparison with terfenadine under physiological conditions. *J. Pharmacol. Exp. Ther.* **2000**, *292*, 261–264.

(41) Katayama, Y.; Fujita, A.; Ohe, T.; Findlay, I.; Ruachi, Y. Inhibitory effects of vesnarinone on cloned cardiac delayed rectifier K⁺ channels expressed in a mammalian cell line. *J. Pharmacol. Exp. Ther.* **2000**, *294*, 339–346.

(42) Kim, K.-S.; Kim, E.-J. The phenothiazine drugs inhibit hERG potassium channels. *Drug Chem. Toxicol.* **2005**, *28*, 303–313.

(43) Kuryshv, Y. A.; Brown, A. M.; Wang, L.; Benedict, C. R.; Rampe, D. Interactions of the 5-hydroxytryptamine 3 antagonist class of antiemetic drugs with human cardiac ion channels. *J. Pharmacol. Exp. Ther.* **2000**, *295*, 614–620.

(44) Sanchez-Chapula, J. A.; Ferrer, T.; Navarro-Polanco, R. A.; Sanguinetti, M. C. Voltage-dependent profile of human *Ether-a-go-go*-related gene channel block is influenced by a single residue in the S6 transmembrane domain. *Mol. Pharmacol.* **2003**, *63*, 1051–1058.

(45) Teschemacher, A. G.; Seward, E. P.; Hancox, J. C.; Witchel, H. J. Inhibition of the current of heterologously expressed hERG potassium

channels by imipramine and amitriptyline. *Br. J. Pharmacol.* **1999**, *128*, 479–485.

(46) Tie, H.; Walker, B. D.; Singleton, C. B.; Valenzuela, S. M.; Bursill, J. A.; Wyse, K. R.; Breit, S. N.; Campbell, T. J. Inhibition of hERG potassium channels by the antimalarial agent halofantrine. *Br. J. Pharmacol.* **2000**, *130*, 1967–1975.

(47) Walker, B. D.; Valenzuela, S. M.; Singleton, C. B.; Tie, H.; Bursill, J. A.; Wyse, K. R.; Qiu, M. R.; Breit, S. N.; Campbell, T. J. Inhibition of hERG channels stably expressed in a mammalian cell line by the antianginal agent perhexiline maleate. *Br. J. Pharmacol.* **1999**, *127*, 243–251.

(48) Zhang, S.; Rajamani, S.; Chen, Y.; Gong, Q.; Rong, Y.; Zhou, Z.; Ruoho, A.; January, C. T. Cocaine blocks hERG, but not KvLQT1+minK, potassium channels. *Mol. Pharmacol.* **2001**, *59*, 1069–1076.

(49) Zhang, S.; Zhou, Z.; Gong, Q.; Makielski, J. C.; January, C. T. Mechanism of block and identification of the verapamil binding domain to hERG potassium channels. *Circ. Res.* **1999**, *84*, 989–998.

(50) Aronov, A. M. Predictive in silico modeling for hERG channel blockers. *Drug Discovery Today* **2005**, *10*, 149–155.

(51) de Bruin, M. L.; Pettersson, M.; Meyboon, R. H. B.; Hoes, A. W.; Leufkens, H. G. M. Anti-HERG activity and the risk of drug-induced arrhythmias and sudden death. *Eur. Heart J.* **2005**, *26*, 590–597.

(52) Baburin, I.; Beyl, S.; Hering, S. Automated fast perfusion of *Xenopus* oocytes for drug screening. *Pflugers Arch.* **2006**, *453*, 117–123.

(53) Milligan, C. J.; Li, J.; Sukumar, P.; Majeed, Y.; Dallas, M. L.; English, A.; Emery, P.; Porter, K. E.; Smith, A. M.; McFadzean, I.; Beccano-Kelly, D.; Bahnasi, Y.; Cheong, A.; Naylor, J.; Zeng, F.; Liu, X.; Gamper, N.; Jiang, L. H.; Pearson, H. A.; Peers, C.; Robertson, B.; Beech, D. J. Robotic multiwell planar patch-clamp for native and primary mammalian cells. *Nat. Protoc.* **2009**, *4*, 244–255.

(54) Polonchuk, L. Toward a new gold standard for early safety: Automated temperature-controlled hERG test on the PatchLiner. *Front. Pharmacol.* **2012**, *3*, 1–7.

(55) Jenks, C. W. Extraction studies of *Tabernanthe iboga* and *Voacanga africana*. *Nat. Prod. Lett.* **2002**, *16*, 71–76.

(56) Koenig, X.; Kovar, M.; Rubi, L.; Mike, A. K.; Lukacs, P.; Gawali, V. S.; Todt, H.; Hilber, K.; Sandtner, W. Anti-addiction drug ibogaine inhibits voltage-gated ionic currents: A study to assess the drug's cardiac ion channel profile. *Toxicol. Appl. Pharmacol.* **2013**, *273*, 259–268.

(57) Vuorinen, A.; Nashev, L. G.; Odermatt, A.; Rollinger, J. M.; Schuster, D. Pharmacophore model refinement for 11 β -hydroxysteroid dehydrogenase inhibitors: Search for modulators of intracellular glucocorticoid concentrations. *Mol. Inf.* **2014**, *33*, 15–25.

(58) Klon, A. E. Machine learning algorithms for the prediction of hERG and CYP450 binding in drug development. *Exp. Opin. Drug Metab. Toxicol.* **2010**, *6*, 821–833.

(59) Hawkins, P. C.; Nicholls, A. Conformer generation with OMEGA: Learning from the data set and the analysis of failures. *J. Chem. Inf. Model.* **2012**, *52*, 2919–2936.

(60) Hawkins, P. C.; Skillman, A. G.; Warren, G. L.; Ellingson, B. A.; Stahl, M. T. Conformer generation with OMEGA: Algorithm and validation using high quality structures from the Protein Databank and Cambridge Structural Database. *J. Chem. Inf. Model.* **2010**, *50*, 572–584.

(61) OMEGA, version 2.3.3; OpenEye Scientific Software: Santa Fe, NM, 2009–2013.

(62) Gaulton, A.; Bellis, L. J.; Bento, A. P.; Chambers, J.; Davies, M.; Hersey, A.; Light, Y.; McGlinchey, S.; Michalovich, D.; Al-Lazikani, B.; Overington, J. P. ChEMBL: A large-scale bioactivity database for drug discovery. *Nucleic Acids Res.* **2012**, *40*, D1100–D1107.

(63) Dunlop, J.; Bowlby, M.; Peri, R.; Vasilyev, D.; Arias, R. High-throughput electrophysiology: An emerging paradigm for ion-channel screening and physiology. *Nat. Rev. Drug Discovery* **2008**, *7*, 358–368.

(64) Coon, T.; Moree, W. J.; Li, B.; Yu, J.; Zamani-Kord, S.; Malany, S.; Santos, M. A.; Hernandez, L. M.; Petroski, R. E.; Sun, A.; Wen, J.;

Sullivan, S.; Haelewyn, J.; Hedrick, M.; Hoare, S. J.; Bradbury, M. J.; Crowe, P. D.; Beaton, G. Brain-penetrating 2-aminobenzimidazole H₁-antihistamines for the treatment of insomnia. *Bioorg. Med. Chem. Lett.* **2009**, *19*, 4380–4384.

(65) Lin, H.; Yamashita, D. S.; Xie, R.; Zeng, J.; Wang, W.; Leber, J.; Safonov, I. G.; Verma, S.; Li, M.; Lafrance, L.; Venslavsky, J.; Takata, D.; Luengo, J. I.; Kahana, J. A.; Zhang, S.; Robell, K. A.; Levy, D.; Kumar, R.; Choudhry, A. E.; Schaber, M.; Lai, Z.; Brown, B. S.; Donovan, B. T.; Minthorn, E. A.; Brown, K. K.; Heerding, D. A. Tetrasubstituted pyridines as potent and selective AKT inhibitors: Reduced CYP450 and hERG inhibition of aminopyridines. *Bioorg. Med. Chem. Lett.* **2010**, *20*, 684–688.

(66) Moree, W. J.; Jovic, F.; Coon, T.; Yu, J.; Li, B. F.; Tucci, F. C.; Marinkovic, D.; Gross, R. S.; Malany, S.; Bradbury, M. J.; Hernandez, L. M.; O'Brien, Z.; Wen, J.; Wang, H.; Hoare, S. R.; Petroski, R. E.; Sacca, A.; Madan, A.; Crowe, P. D.; Beaton, G. Novel benzothiophene H₁-antihistamines for the treatment of insomnia. *Bioorg. Med. Chem. Lett.* **2010**, *20*, 2316–2320.

(67) Webb, R. L.; Schiering, N.; Sedrani, R.; Maibaum, J. Direct renin inhibitors as a new therapy for hypertension. *J. Med. Chem.* **2010**, *53*, 7490–7520.

(68) Park, S. J.; Buschmann, H.; Bolm, C. Bioactive sulfoximines: Syntheses and properties of Vioxx analogs. *Bioorg. Med. Chem. Lett.* **2011**, *21*, 4888–4890.

(69) Schuster, D.; Laggner, C.; Steindl, T. M.; Paluszczak, A.; Hartmann, R. W.; Langer, T. Pharmacophore modeling and in silico screening for new P450 19 (aromatase) inhibitors. *J. Chem. Inf. Model.* **2006**, *46*, 1301–1311.

(70) Wolber, G.; Dornhofer, A. A.; Langer, T. Efficient overlay of small organic molecules using 3D pharmacophores. *J. Comput.-Aided Mol. Des.* **2006**, *20*, 773–788.

(71) Seidel, T.; Ibis, G.; Bendix, F.; Wolber, G. Strategies for 3D pharmacophore-based virtual screening. *Drug Discovery Today: Technol.* **2010**, *7*, e221–e228.

(72) Li, H.; Sutter, J.; Hoffmann, R. HypoGen: An Automated System for Generating 3D Predictive Pharmacophore Models. In *Pharmacophore Perception, Development, and Use in Drug Design*; Güner, O. F., Ed.; International University Line: La Jolla, CA, 2000; pp 172–189.

(73) Stork, D.; Timin, E. N.; Berjukow, S.; Huber, C.; Hohaus, A.; Auer, M.; Hering, S. State dependent dissociation of HERG channel inhibitors. *Br. J. Pharmacol.* **2007**, *151*, 1368–1376.

(74) Windisch, A.; Timin, E.; Schwarz, T.; Stork-Riedler, D.; Erker, T.; Ecker, G.; Hering, S. Trapping and dissociation of propafenone derivatives in HERG channels. *Br. J. Pharmacol.* **2011**, *162*, 1542–1552.